Selective Growth of Fullerenes from C60 to C70: Inherent Geometrical Connectivity Hidden in Discrete Experimental Evidence

ARTICLE *in* THE JOURNAL OF PHYSICAL CHEMISTRY C · JANUARY 2013

Impact Factor: 4.77 · DOI: 10.1021/jp3100766

5 AUTHORS, INCLUDING:

Jia Zheng
Henan University
23 PUBLICATIONS **148** CITATIONS
SEE PROFILE

Xiang Zhao
Xi'an Jiaotong University
130 PUBLICATIONS **1,247** CITATIONS
SEE PROFILE

THE JOURNAL OF PHYSICAL CHEMISTRY C

Article

pubs.acs.org/JPCC

Selective Growth of Fullerenes from C_{60} to C_{70}: Inherent Geometrical Connectivity Hidden in Discrete Experimental Evidence

Wei-Wei Wang,[†,§] Jing-Shuang Dang,[†,§] Jia-Jia Zheng,[†] Xiang Zhao,*[,†] and Shigeru Nagase[‡]

[†]Institute for Chemical Physics & Department of Chemistry, State Key Laboratory of Electrical Insulation and Power Equipment, Xi'an Jiaotong University, Xi'an 710049, China

[‡]Fukui Institute for Fundamental Chemistry, Kyoto University, Kyoto 606-8103, Japan

Supporting Information

ABSTRACT: The bottom-up growth mechanism of fullerenes in the range of C_{60}-C_{70} has been studied step by step, and a novel growth pathway was put forward for the first time. Analysis on geometrical connectivity indicates that almost all of the synthesized pristine C_{60}-C_{70} fullerenes participate in the growth channel, and those molecules are linked by simple and successive C_2 insertion reactions, implying that the formation of fullerene is not a random but certain event and those experimental findings are not discrete but related to each other. In energy, except for one step of unavoidable isomerization from C_{68} to C_{70}, density functional theory calculations indicate that the growth processes are exothermic with low energy barriers (<3 eV). Kinetically, the reaction rate for each step was estimated, and the results demonstrate that addition reactions easily to occur at elevated temperatures.

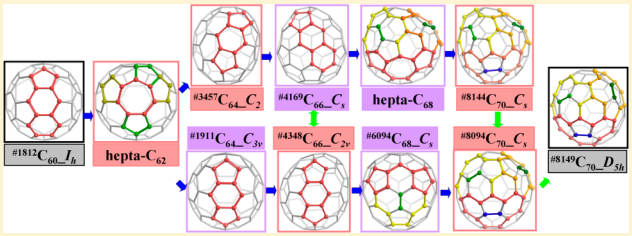

1. INTRODUCTION

Ever since the discovery of I_h-symmetric C_{60}, numerous experimental and theoretical efforts have been devoted to find new fullerene structures for the design of functionalized carbon materials on the nanoscale.[1,2] However, owing to the "energy penalty" caused by adjacent pentagons, only a few of IPR (isolated pentagon rule)-obeying hollow cages have hitherto been successfully synthesized and characterized, such as $^{\#1812}C_{60}\_I_h$ and $^{\#8149}C_{70}\_D_{5h}$.[3] In the past decade, exohedral chlorination has been received as an effective approach to yield the fullerene derivatives. A series of experiments demonstrate that the pristine cage-like molecules can be stabilized and captured by assembling with the adatoms on reactive sites. Since the first chlorinated fullerene derivative $C_{50}Cl_{10}$ was synthesized in milligram quantities,[4] more and more unconventional IPR-violating fullerenes were obtained by this method.[5−16] Energetically, those isolated carbon cages include not only the thermodynamic stable structures that have been predicted in theory but also some unexpected thermo-unfavorable species. Accordingly, the diversity of the fullerene family has been expanded enormously. However, with the discovery of chlorofullerenes in various sizes (from C_{50} to C_{96}),[4−17] some deeper problems emerge. For example, are those fullerene derivatives produced in a stochastic way or of inevitability? Are those carbon cages discrete or related to each other? How does one explain the formation of thermodynamically unfavorable fullerenes,[7,15] such as the pineapple-like C_{64}? Besides those existing reports, are there any unidentified fullerenes from the graphite arc plasma?

Naturally, the only way to elucidate those questions is to uncover the fullerene formation and growth mechanism. In theory, many hypothetical predictions were proposed to describe the growth pathway of fullerenes in the last 25 years.[18−25] In recent years, a so-called "bottom-up" model is widely accepted because of support from experimental findings as well as the quantum chemical molecular dynamics (QM/MD) simulations.[16,25] In the bottom-up growth road, a smaller fullerene (C_n) is served as the parent molecule that can assemble with the external carbon dimer to change into a larger closed cage C_{n+2}.[26−31] Likewise, the produced C_{n+2} is capable of reacting with the C_2 group continuously to yield a larger C_{n+4}. Accordingly, a series of addition products in ascending sizes can be obtained from the graphite plasma at high temperatures.[11,16,25] In our previous work, the selective growth process of small fullerenes (no larger than C_{60}) was studied based on this size-up growth model.[31] Moreover, the unity of thermodynamic and kinetic control in C_2 insertion reaction was proved, and an optimal growth route was proposed for small fullerenes. However, thus far, our prediction is still difficult to testify due to the extreme instability of small fullerenes.

Compared with small carbon cages, pristine fullerenes in medium size (C_{60}-C_{70}) are easier to be stabilized by external halogen atoms and generate various exohedral complexes because of the larger cage size and smaller strain energy. $^{\#1911}C_{64}Cl_4$, $^{\#1911}C_{64}Cl_8$, $^{\#4169}C_{66}Cl_6$, $^{\#4169}C_{66}Cl_{10}$, $^{\#6094}C_{68}Cl_8$, and a heptagon-incorporating $C_{68}Cl_6$ have been successively identified in the laboratory, and these experimental outcomes provide essential support for further investigations on the

Received: October 11, 2012
Revised: January 10, 2013
Published: January 10, 2013

   dx.doi.org/10.1021/jp3100766 | J. Phys. Chem. C 2013, 117, 2349−2357

fullerene growth mechanism.[7,11,13,15,16] Moreover, $^{\#1812}C_{60}\_I_h$ and $^{\#8149}C_{70}\_D_{5h}$ are the two most abundant and widely applied IPR structures in the field of fullerene study,[1] but the detailed growth processes of the two molecules, including the selectivity of mechanisms, the rational intermediates along the growth routes, and the energy barrier for each step, are barely reported.

Herein, by means of geometrical connectivity analysis and density functional theory (DFT) kinetic calculations, the fullerene growth mechanism from C_{60} to C_{70} has been investigated for the first time. Starting from the IPR-obeying C_{60}, we find that these identified pristine cages form a novel growth channel with low energy barriers through sequential insertion of C_2 clusters. In addition, some hitherto unidentified but kinetically rational fullerene structures are discovered in this work. The outcomes provide precise theoretical predictions on the formation mechanism of fullerenes and give a novel insight into the selective synthesis of fullerenes in experiments.

2. THEORETICAL CALCULATIONS

All calculations were performed using the Gaussian09 program package.[32] Full geometry optimizations on all of relevant structures (reactants, products, intermediates and transition states) were carried out using Becke's three-parameter exchange functional with the correlation functional of Lee, Yang, and Parr (B3LYP) and the standard 6-31G(d) basis set.[33−35] The B3LYP functional was chosen because it is the most popular functional in fullerene scope in the past decade. Besides, to identify the influence of different density functional methods, we calculated the addition reaction $C_{60} + C_2 \rightarrow C_{62}$ by using both the B3LYP and M06-2X[36] functionals, and it turned out that the energy barriers of C_{60}-C_{62} with the two different levels (M06-2X/6-31G(d) and B3LYP/6-31G(d)) are quite close (2.95 eV for B3LYP versus 2.97 eV for M06-2X), suggesting that the functional of B3LYP is reliable for investigations on fullerene growth reactions. In this report, $^{\#y}C_x_$symm denotes each classical fullerene molecule, where x signifies the number of carbon atoms, y is used to denote its corresponding spiral code,[37] and symm represents the point group symmetry. To clarify the nature of stationary points as global minima or transition states with one imaginary frequency, we conducted vibrational frequency analyses at the same DFT level of theory as geometry optimizations. Kinetically, on the basis of the transition state theory (TST), the reaction rates can be obtained by the Arrhenius formula: $\nu \exp(-E_b/k_BT)$, where ν is the attempt frequency, T is the reaction temperature, E_b is the computed energy barrier, and k_B is the Boltzmann constant. Herein the reaction rates for all additions and rearrangements are calculated, and the reaction temperature is considered to be 2500 K because the temperature range for fullerene growth has been estimated to be about 2000−2500 K.[16]

3. RESULTS AND DISCUSSION

Fullerene growth includes the increase in carbon atoms and the skeletal isomerization. Herein two essential chemical reactions during the fullerene formation, C_2 addition and Stone−Wales transformation (SWT),[27,38] were discussed in the first part. Figure 1a illustrates the original model of C_2 addition reaction, which was proposed by Endo and Kroto in 1992.[27] Whereas a C_2 cluster is inserted at the para positions of a hexagonal ring, two fused pentagonal rings are yielded. It is apparent that the limitation of this model lies in the inevitable pentagon pair, which violates the well-recognized IPR. To elucidate the formation of IPR fullerenes and some nonclassical fullerenes with four or seven-membered rings,[39] the original model was generalized subsequently. As shown in Figure 1b, the cycles in the black dotted line denote the carbon rings in the reactant, and the number in each ring indicates the size of the carbocyclic ring (including 4,5,6,7-membered rings). After the insertion of C_2 unit, the sizes of two bilateral rings are enlarged into **n**+1 and **l**+1, respectively. Meanwhile, the middle carbon ring **m** is separated into two parts, denoted by $\mathbf{m}_1$ and $\mathbf{m}_2$ separately. Obviously, it could be concluded that $(\mathbf{m}_1 - 2) + (\mathbf{m}_2 - 2) = \mathbf{m}$. For example, if **n** or **l** represents the hexagon, then a nonclassical heptagon-containing product will be obtained after the C_2 insertion. Besides, while **m** = 7, the heptagon will change into a pentagon−hexagon pair after addition. This model successfully refrains from the appearance of pentagon pairs and is widely used to explain the generation of IPR structures. We found that with difference from the growth of small fullerenes, enlargement of fullerenes in a larger size (beyond C_{60}) contains multiple kinds of addition models, and accordingly the Endo−Kroto patch is no longer the solo feasible mechanism. Each step of C_2 addition will be discussed below in detail.

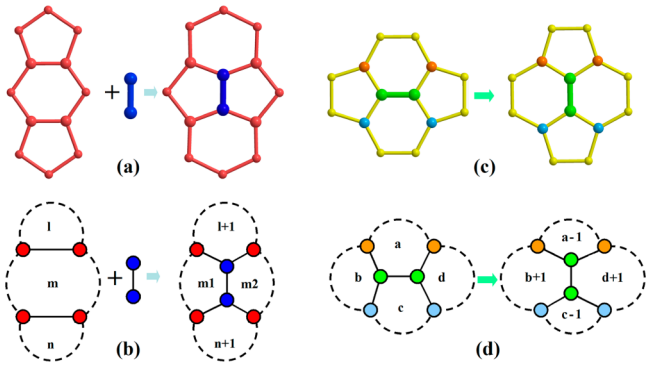

Figure 1. Original and generalized mechanisms of C_2 insertion and Stone−Wales transformation.

Besides the C_2 insertion modeling, Stone−Wales transformation is another chemical reaction that connects two isolated carbon cages. Figure 1c exhibits the original model of SWT, which was presented by Stone and Wales in 1986.[38] By rotating the [6,6] conjunction bond of the pyracylene-like fragment, $^{\#1812}C_{60}\_I_h$ can be isomerized with $^{\#1809}C_{60}\_C_{2v}$ reciprocally. Later, to explain the formation of some other defective fragments in nanocarbon materials, the generalized SWT (GSWT) was proposed by Ōsawa and coworkers.[40] As illustrated in Figure 1d, by rotating the center bond of the reaction area, the generation or elimination of carbon rings in multiple sizes is successfully elucidated in theory. However, compared with the C_2 addition reaction, SWT or GSWT behaves with a much larger energy requirement (the energy barrier is in the range of 5−7 eV).[41−45] Accordingly, from the viewpoint of kinetics, a practicable growth route should avoid the reconstruction reactions whenever possible. In the following sections, based on the above-mentioned two chemical reactions, the growth of fullerenes from C_{60} to C_{70} will be studied step by step at the DFT level of theory. It should be noted that although each fullerene surface includes several addition sites, only those active sites related to special growth processes toward the experimentally identified or energetically favored products have been taken into account in this work. Our aim is to uncover the geometrical connections between

dx.doi.org/10.1021/jp3100766 | J. Phys. Chem. C 2013, 117, 2349−2357

cages and find an optimal growth pathway that is favorable both thermodynamically and kinetically.

C_{60}-C_{62}: Decomposing of IPR Fullerene. Because diverse C_{60} isomeric origins give rise to different growth routes, herein the IPR-$^{\#1812}C_{60}\_I_h$ was selected as the starting point of the growth because of its significant role in fullerene scope. Structurally, due to the unique symmetrical characteristic of $^{\#1812}C_{60}\_I_h$, the corresponding C_2 addition products are two nonclassical structures (a tetragon-containing C_{62} and a heptagon-incorporating one, as shown in Figure 2). Note that

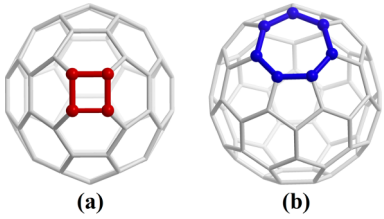

Figure 2. Two stable nonclassical C_{62} isomers. (a) hepta-C_{62} and (b) tetra-C_{62}.

although the C_{62} with a square was synthesized by chemical approaches, so far there is still no experimental evidence proving that C_{60} is capable of assembling with the dissociated C_2 dimer from a graphite plasma to afford this nonclassical fullerene.[46] Energetically, previous DFT calculation indicated that the heptagon-containing C_{62} (hepta-C_{62}) is the ground state of C_{62} in a wide temperature interval (from 0 to 4000 K) based on the equilibrium statistical thermodynamic analyses in terms of Gibbs function.[47] Accordingly, the hepta-C_{62} was supposed to be essential in the C_{60}-C_{70} growth route, and the reaction process of C_{60}-C_{62} (Scheme 1) was studied in detail.

Scheme 1. C_2 Addition from $^{\#1812}C_{60}\_I_h$ to Hepta-C_{62}[a,b]

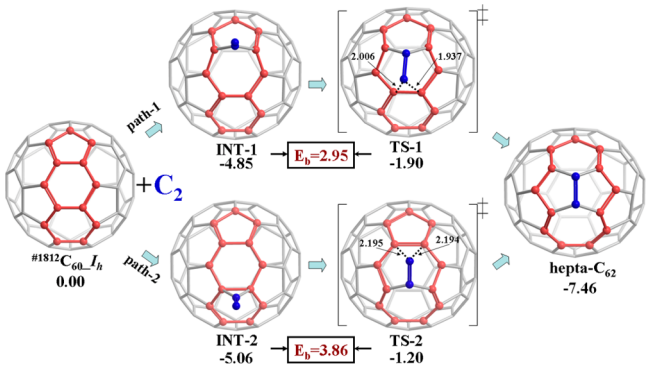

[a] E_b indicates the energy barrier. [b] Energies are given in eV, and C−C distances are in units of Å.

As illustrated in Scheme 1, the C_{60}-C_{62} enlargement process takes place on a 5/6/6 fragment of C_{60} surface. The initial step of C_2 addition is that one atom of the C_2 cluster is attaching onto the carbon cage and meanwhile the other one is dangling to generate a stick-like intermediate, which is a barrierless process. Note that the stick adduct was discovered by using high-resolution ion-mobility measurements experimentally,[26] which provides strong evidence to support the rationality of the mechanism. According to the diverse addition sites ([5,6] or [6,6] conjunction on fragment 5/6/6), C_2 insertion is sorted into two paths (path-1 and path-2 in Scheme 1). In the second step, the unsaturated atom of the intermediate begins to close to the fullerene surface. It could be concluded from the potential energy surface (PES) survey that this is an unsynchronized process. The unsaturated atom does not bond with the two atoms simultaneously but moves toward one first to form a sp^3 structure. A transition state (TS) can be located between the stick-like intermediate and the sp^3 structure. This course is similar to those of small fullerenes.[31] The sp^3 structure, although which could not be located at various DFT levels, is widely regarded as a significant state in the fullerene growth.[31,48] Energetically, the singlet−triplet splitting energies ($\Delta E_{st} = E_{triplet} - E_{singlet}$) of both $^{\#1812}C_{60}\_I_h$ and hepta-C_{62} are 1.67 and 0.32 eV, respectively, and the addition process was consequently simulated in the closed-shell singlet state. As shown in Table 1, the stick-like intermediate in path-2 is 0.21 eV more favorable than that in path-1, indicating that C_2 dimer holds a little stronger adsorption on the [6,6] adjacency than the [5,6] pair in $^{\#1812}C_{60}\_I_h$. However, the energy barriers of C_2 insertion on $^{\#1812}C_{60}\_I_h$ are 2.95 and 3.86 eV for path-1 and path-2, respectively, revealing that path-1 is more kinetically favorable. According to the Arrhenius equation, the calculated reaction rate at 2500 K along the path-1 is 1.6×10^7 s^{-1} in comparison with 1.3×10^5 s^{-1} of the path-2. Consequently, it seems that C_2 insertion on $^{\#1812}C_{60}\_I_h$ is prone to occur via path-1.

After the enlargement, the IPR structure is changed into a nonclassical fullerene that contains a heptagon and a segment of quadruple sequentially fused pentagons (QSFP). Although this nonclassical fullerene has not been observed experimentally, the existence of this structure may be convinced due to the high thermodynamic stability and low formation barrier. Furthermore, the addition of hepta-C_{62} together with the corresponding C_{64} products that are discussed below will also testify the irreplaceable role of hepta-C_{62} in fullerene growth.

C_{62}−C_{64}: Addition to Heptagonal Ring. Acting as the growth reagent, there are many addition sites on hepta-C_{62}, and among all of those possible addition products, two classical C_{64} isomers are the most noteworthy. As shown in Scheme 2, by ingestion of a C_2 dimer on different sites, the heptagonal ring on hepta-C_{62} is decomposed and two C_{64} isomers ($^{\#3457}C_{64}\_C_2$ and $^{\#1911}C_{64}\_C_{3v}$) can be obtained. Structurally, $^{\#3457}C_{64}\_C_2$ possesses two pentagon pairs that ensure it is one of the three isomers with the lowest number of pentagon pairs (N_{55}) among 3465 classical C_{64} (the other two are $^{\#3451}C_{64}\_D_2$ and $^{\#3452}C_{64}\_C_s$), and hence a relative stability of $^{\#3457}C_{64}\_C_2$ can be predicted. By contrast, because of the structural strain caused by the triple directly fused pentagons (TDFPs), the pristine $^{\#1911}C_{64}\_C_{3v}$ is energetically unfavorable compared with the three isomers with two pentagon pairs. However, to date, $^{\#1911}C_{64}\_C_{3v}$ is the only C_{64} species that was isolated experimentally. In 2008 and 2012, it was captured in the form of $C_{64}Cl_4$ and $C_{64}Cl_8$.[7,15] Since the first TDFP-incorporating exohedral derivatives $C_{64}Cl_4$ was discovered in experiment,[7] there has still been an unsolved question of why a thermodynamically unfavorable carbon cage ($^{\#1911}C_{64}\_C_{3v}$) can be obtained rather than other more stable isomers? In the present work, we manage to clarify the essential reason for the first time. As the addition parent of C_{64} and also the most stable addition product of C_{60}, the existence of hepta-C_{62} determines the formation of this thermo-unfavorable C_{64} ($^{\#1911}C_{64}\_C_{3v}$) by C_2 insertion at high temperatures. Subsequently, it is accepted that the passivation by external chlorine atoms on the active

dx.doi.org/10.1021/jp3100766 | J. Phys. Chem. C 2013, 117, 2349−2357

Table 1. Adsorption Energies (E_{ad}, in eV),[a] Energy Barriers (E_b, in eV),[b] Reaction Energies (E_r, in eV),[c] and Reaction Rates at 2500 K (in s^{-1})[d] for the C_2 Addition Reactions and Stone−Wales Transformations of C_{60}-C_{70}

reaction	path	ΔN_{55}[e]	ΔN_7[e]	E_{ad}	E_b	E_r	reaction rate
$^{\#1812}C_{60}$ → epta-C_{62}	1	3	1	−4.85	2.95	−7.46	1.6×10^7
	2	3	1	−5.06	3.86	−7.46	1.3×10^5
hepta-C_{62} → $^{\#3457}C_{64}$	1	−1	−1	−5.76	1.72	−10.36	2.2×10^9
	2	−1	−1	−5.01	2.30	−10.36	2.7×10^8
hepta-C_{62} → $^{\#1911}C_{64}$		0	−1	−5.36	2.22	−9.71	2.6×10^8
$^{\#3457}C_{64}$ → $^{\#4169}C_{66}$	1	0	0	−5.91	1.57	−10.37	8.6×10^9
	2	0	0	−5.33	1.62	−10.37	6.4×10^9
$^{\#1911}C_{64}$ → $^{\#4348}C_{66}$[f]	1	−1	0	−6.32 (−6.04)	0.97 (1.51)	−10.80 (−10.83)	1.4×10^{11} (1.3×10^{10})
	2	−1	0	−5.47 (−5.30)	0.83 (1.26)	−10.80 (−10.83)	2.8×10^{11} (1.2×10^{10})
$^{\#4169}C_{66}$ → hepta-C_{68}	1	0	1	−5.40	1.94	−10.13	1.5×10^9
	2	0	1	−5.01	2.10	−10.13	7.9×10^8
$^{\#4348}C_{66}$ → $^{\#6094}C_{68}$[f]	1	0	0	−5.37 (−5.47)	0.89 (1.24)	−9.84 (−10.20)	1.7×10^{11} (3.8×10^{10})
	2	0	0	−5.05 (−5.12)	0.91 (1.15)	−9.84 (−10.20)	1.7×10^{11} (5.1×10^{10})
$^{\#4169}C_{66}$ → $^{\#4348}C_{66}$[f]		0	0		6.07 (5.24)	0.22 (−0.68)	8.6 (3.6×10^2)
$^{\#4348}C_{66}$ → $^{\#4169}C_{66}$[f]		0	0		5.89 (5.92)	−0.22 (0.68)	2.4×10^1 (1.5×10^1)
$^{\#6094}C_{68}$ → $^{\#8094}C_{70}$[f]		−1	0	−5.54 (−5.54)	0.68 (1.40)	−11.63 (−10.25)	4.4×10^{11} (1.4×10^{10})
$^{\#8094}C_{70}$ → $^{\#8149}C_{70}$		−1	0		6.00	−1.33	2.6×10^1
hepta-C_{68} → $^{\#8144}C_{70}$		0	−1	−5.23	1.94	−10.24	2.6×10^9
$^{\#8144}C_{70}$ → $^{\#8094}C_{70}$		−1	0		5.89	−0.88	3.9×10^1

[a] $E_{ad} = E(INT) - (E(C_n) + E(C_2))$. [b] $E_b = E(TS) - E(INT)$. [c] $E_r = E(C_{n+2}) - (E(C_n) + E(C_2))$. [d] Reaction rates were calculated based on the Arrhenius formula. [e] ΔN_{55} and ΔN_7 denote the change in number of the pentagon pairs and heptagons after the addition. [f] Reactions $^{\#1911}C_{64}$ → $^{\#4348}C_{66}$, $^{\#4348}C_{66}$ → $^{\#6094}C_{68}$, $^{\#4348}C_{66}$ → $^{\#4169}C_{66}$, $^{\#4169}C_{66}$ → $^{\#4348}C_{66}$, and $^{\#6094}C_{68}$ → $^{\#8094}C_{70}$ were simulated in both singlet and triplet states, and the corresponding E_{ad}, E_b, E_r, and reaction rate in brackets denote the triplet results.

Scheme 2. C_2 Addition from Hepta-C_{62} to $^{\#1911}C_{64}$_C_{3v} and $^{\#3457}C_{64}$_C_2[a,b]

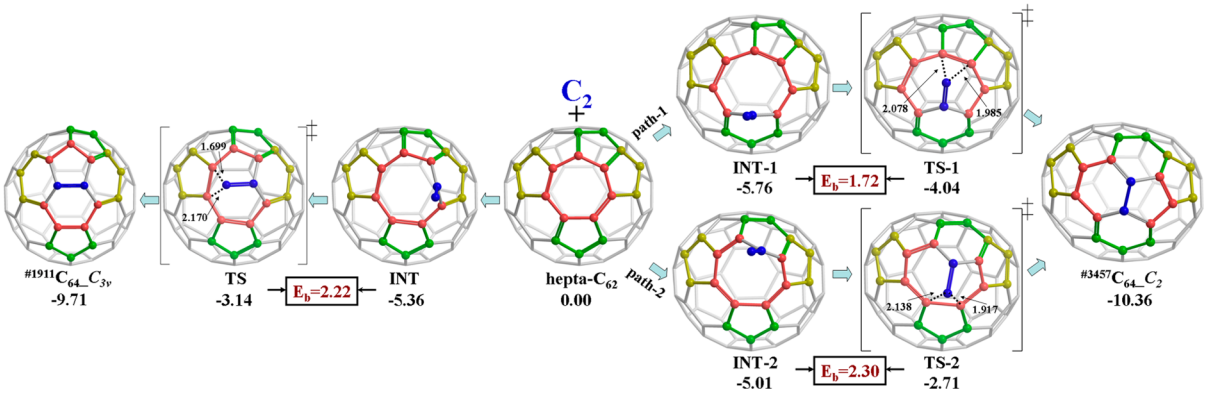

[a] E_b indicates the energy barrier. [b] Energies are given in eV, and C−C distances are in units of Å.

sites during the annealing process gives rise to the pristine cage ($^{\#1911}C_{64}$_C_{3v}) that can be captured in the form of chloride. Therefore, the discovery of $^{\#1911}C_{64}$_C_{3v} is not a random but certain event. $^{\#1911}C_{64}$_C_{3v} serves as an inevitable product during fullerene growth. Additionally, as another direct C_2 insertion product of hepta-C_{62} and also one of the lowest energy C_{64} isomers, we consider that $^{\#3457}C_{64}$_C_2 might be experimentally observed sooner or later. Except for the two classical isomers, the other addition products of hepta-C_{62} all possess more fused pentagon pairs, and hence we did not study the addition processes toward those isomers.

The kinetic processes toward $^{\#1911}C_{64}$_C_{3v} and $^{\#3457}C_{64}$_C_2 are illustrated in Scheme 2. Because the ground state of hepta-C_{62} is singlet, the two processes were examined in the single PES. Similar with the addition on $^{\#1812}C_{60}$_I_h, the first step is the formation of a stick-like intermediate on the [5,7] conjunction bond. In the case of the production of $^{\#1911}C_{64}$_C_{3v}, the two [5,7] bonds are totally equivalent, which results in a unique addition route. After overcoming an asynchronous transition state, the heptagon is divided into a pentagon-hexagon pair and finally the product is formed. The energy barrier of this process is 2.22 eV. As for the generation of $^{\#3457}C_{64}$_C_2, due to the different chemical environment around the two [5,7] bonds, the addition course affords two stick-like intermediates, which correspond to two distinct reaction routes. As shown in Scheme 2, energetically, because path-1 holds a more stable intermediate and a lower energy barrier than path-2 (1.72 eV for path-1, 2.30 eV for path-2), path-1 is a more proper addition pathway from both the kinetic and thermodynamic considerations. Compared with the addition on $^{\#1812}C_{60}$_I_h, a more negative reaction energy for the formation of the stick-like intermediate demonstrate that hepta-C_{62} is easier to adsorb the external C_2 cluster to form a stable intermediate. Moreover, the energy barriers for the

dx.doi.org/10.1021/jp3100766 | J. Phys. Chem. C 2013, 117, 2349−2357

formation of $^{\#1911}C_{64}\_C_{3v}$ and $^{\#3457}C_{64}\_C_2$ are much smaller than that of hepta-C_{62}. On the basis of the Arrhenius formula, the reaction rates toward both $^{\#1911}C_{64}\_C_{3v}$ and $^{\#3457}C_{64}\_C_2$ at 2500 K are 2.7×10^8 and 2.2×10^9 s^{-1}, respectively. Accordingly, it is predictable that the heptagon-incorporating C_{62} that derives from $^{\#1812}C_{60}\_I_h$ at high temperatures is easy to react with C_2 to generate the larger cages, which might be the explanation for the insufficiency of the experimental information for hepta-C_{62}.

C_{64}–C_{66}: Endo–Kroto Enlargement. The enlargement process from C_{64} to C_{66} is divided into two separate paths because two different classical C_{64} isomers ($^{\#3457}C_{64}\_C_2$ and $^{\#1911}C_{64}\_C_{3v}$) are generated from hepta-C_{62}. On the basis of the geometrical analysis, whereas $^{\#3457}C_{64}\_C_2$ is acting as a reactant of growth, the lowest energy structure among all addition products is a classical fullerene $^{\#4169}C_{66}\_C_s$, which is obtained by the addition on the 5/6/5 Endo–Kroto patch. $^{\#4169}C_{66}\_C_s$, whose derivatives ($^{\#4169}C_{66}Cl_6$ and $^{\#4169}C_{66}Cl_{10}$) have been reported experimentally, possesses a triple sequentially fused pentagons (TSFP) fragment in its geometrical configuration.[11] Moreover, for the C_s symmetric $^{\#4169}C_{66}\_C_s$, the two [5,5] conjunctions are completely symmetrical. Hence $^{\#3457}C_{64}\_C_2$ is the only possible C_2 addition parent (or C_2 ejection product) for $^{\#4169}C_{66}\_C_s$, suggesting that although it has not been reported experimentally as an important intermediate, $^{\#3457}C_{64}\_C_2$ plays an irreplaceable role in the fullerene growth. Kinetically, the C_2 insertion toward $^{\#4169}C_{66}\_C_s$ follows the classical addition model on fragment 5/6/5. As shown in Scheme 3, two addition pathways were considered on the basis

Scheme 3. C_2 Addition from $^{\#3457}C_{64}\_C_2$ to $^{\#4169}C_{66}\_C_s$[a,b]

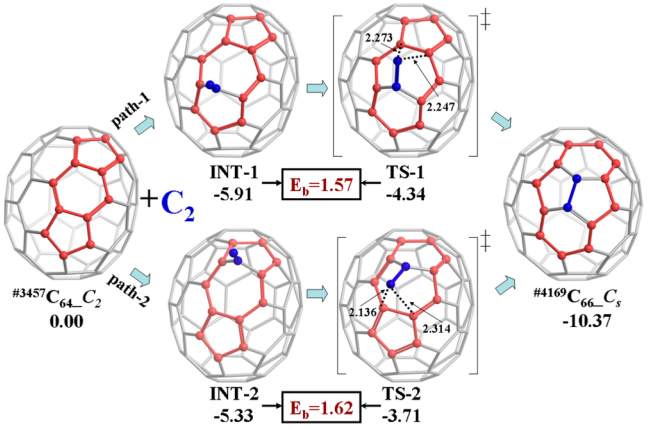

[a]E_b indicates the energy barrier. [b]Energies are given in eV, and C–C distances are in units of Å.

of different adsorption sites. Moreover, calculations at the B3LYP/6-31G(d) level indicate that singlet–triplet splitting energies ΔE_{st} for $^{\#3457}C_{64}\_C_2$ and $^{\#4169}C_{66}\_C_s$ are 0.78 and 0.86 eV, respectively, and the growth from $^{\#3457}C_{64}\_C_2$ to $^{\#4169}C_{66}\_C_s$ was accordingly simulated via singlet PES survey. The path-1 needs to overcome a slightly lower energy barrier than path-2 (1.57 eV for path-1, and 1.62 eV for path-2), and the intermediate formed in the first step of path-1 is energetically 0.58 eV lower than that of path-2. Therefore, path-1 serves as a more favorable reaction route during the growth from $^{\#3457}C_{64}\_C_2$ to $^{\#4169}C_{66}\_C_s$, and the calculated reaction rate at 2500 K is 8.6×10^9 s^{-1}.

In the case of $^{\#1911}C_{64}\_C_{3v}$, the C_{3v}-symmetric structure has three equivalent 5/6/5 fragments, so only one classical C_{66} product can be obtained via C_2 addition. As illustrated in Scheme 4, after the addition on $^{\#1911}C_{64}\_C_{3v}$, the configuration

Scheme 4. C_2 Addition from $^{\#1911}C_{64}\_C_{3v}$ to $^{\#4348}C_{66}\_C_{2v}$[a,b,c]

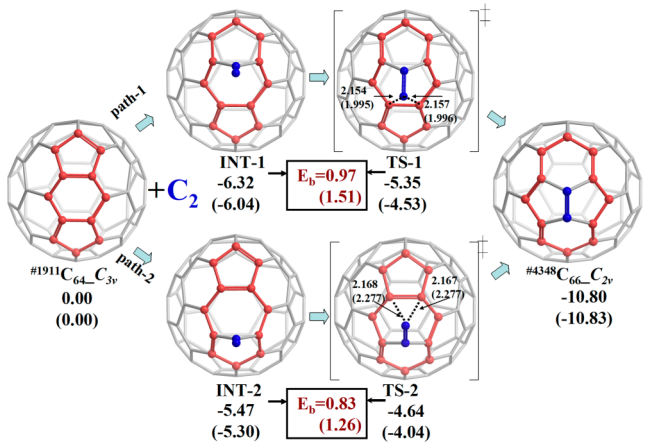

[a]E_b indicates the energy barrier. [b]Energies are given in eV, and C–C distances are in units of Å. [c]Energies and bond distances in brackets denote the triplet results.

of TDFP vanishes, and meanwhile N_{55} is reduced to two. The corresponding adduct is $^{\#4348}C_{66}\_C_{2v}$, one of three C_{66} isomers with the lowest fused pentagons (the other two are $^{\#4169}C_{66}\_C_s$ and $^{\#4466}C_{66}\_C_2$). Meanwhile, $^{\#4348}C_{66}\_C_{2v}$ is also the most stable product of C_2 insertion from $^{\#1911}C_{64}\_C_{3v}$. Interestingly, although hitherto there is still no experimental information about its external derivative, $^{\#4348}C_{66}\_C_{2v}$ has already been synthesized in the form of endohedral metallofullerene $Sc_2@C_{66}$.[49] It is known that passivation by halogens and encapsulating with metal atoms are the two main approaches to obtain fullerene derivatives, and the similarity between the two methods is that the structural and electronic characteristics are altered by assembling with foreign atoms or clusters so that the active sites in the carbon sphere are stabilized. We believe that our study not only is conducive to find new fullerene external derivatives but also supplies a new insight into understanding the formation mechanism of endohedral metallofullerenes. Similar to the addition on $^{\#3457}C_{64}\_C_2$, the reaction from $^{\#1911}C_{64}\_C_{3v}$ to $^{\#4348}C_{66}\_C_{2v}$ (on the fragment of 5/6/5) is also an enlargement between classical fullerenes. Interestingly, optimizations on the different spin states demonstrate that electronic ground states of both $^{\#1911}C_{64}\_C_{3v}$ and $^{\#4348}C_{66}\_C_{2v}$ are two unexpected triplet states, and the splitting energies are very small (−0.01 eV for $^{\#1911}C_{64}\_C_{3v}$ and −0.03 eV for $^{\#4348}C_{66}\_C_{2v}$), implying that the singlet–triplet conversion of such two structures may readily occur at elevated temperatures. Therefore, the C_2 addition process from $^{\#1911}C_{64}\_C_{3v}$ to $^{\#4348}C_{66}\_C_{2v}$ has been investigated in both singlet and triplet states in this work. As exhibited in Scheme 4, the addition is sorted into two reaction routes. In energy, path-1 holds more stable intermediates and transition states, which reveals that path-1 is a more suitable reaction route in practice. Moreover, the reaction barriers in singlet and triplet PESs along path-1 are 0.97 and 1.51 eV, indicating that the growth from $^{\#1911}C_{64}\_C_{3v}$ to $^{\#4348}C_{66}\_C_{2v}$ is very likely to occur in singlet PES, with a reaction rate of 1.4×10^{11} s^{-1}.

dx.doi.org/10.1021/jp3100766 | J. Phys. Chem. C 2013, 117, 2349–2357

According to the above kinetic analyses on the growth from C_{62} to C_{66}, it is worth noting that compared with $^{\#1911}C_{64}$, $^{\#3457}C_{64}$ possesses a faster reaction rate to form from the hepta-C_{62} and a higher barrier to transform to C_{66}. Therefore, $^{\#3457}C_{64}$ exhibits a better kinetic stability and should have a greatly higher lifetime than $^{\#1911}C_{64}$, but why is $^{\#1911}C_{64}$ the only C_{64} species identified in experiments so far? We consider that this may be because $^{\#1911}C_{64}$ was captured as a chloride rather than a pristine cage. Because of the high-strain TDFP fragment in the surface, the chlorine atoms are preferred to react with $^{\#1911}C_{64}$ to generate the solid C−Cl bonds and stable chloride. As the other addition product of hepta-C_{62}, $^{\#3457}C_{64}$ is certainly believed to be synthesized in a certain form sooner or later.

Besides the growth connections between the selected C_{64} and C_{66} ($^{\#3457}C_{64}\_C_2$ to $^{\#4169}C_{66}\_C_s$, and $^{\#1911}C_{64}\_C_{3v}$ to $^{\#4348}C_{66}\_C_{2v}$), the geometrical relation between $^{\#4348}C_{66}\_C_{2v}$ and $^{\#4169}C_{66}\_C_s$ was also uncovered. As illustrated in Scheme 5,

Scheme 5. Stone−Wales Transformation between $^{\#4169}C_{66}\_C_s$ and $^{\#4348}C_{66}\_C_{2v}$[a,b]

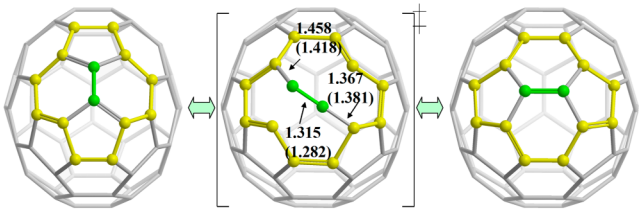

[a]Energies are given in eV, and C−C distances are in units of Å. [b]Energies and bond distances in brackets denote the triplet results.

by one step of SWT, isomers $^{\#4348}C_{66}\_C_{2v}$ and $^{\#4169}C_{66}\_C_s$ can be interchanged. The energy barriers of the SWT from $^{\#4348}C_{66}\_C_{2v}$ to $^{\#4169}C_{66}\_C_s$ are 5.89 eV (6.07 eV for the reverse reaction) in the singlet state and 5.92 eV (6.10 eV toward the reverse direction) in the triplet state, respectively. Although the activation requirements of the SWT between $^{\#4348}C_{66}\_C_{2v}$ and $^{\#4169}C_{66}\_C_s$ are much larger than those of growth reactions, the calculated reaction rates listed in Table 1 prove that such carbon skeletal rearrangements are possible at elevated temperatures.

C_{66}−C_{68}: Yield of the Classical and Heptagon-Containing C_{68}. Sequentially, both $^{\#4169}C_{66}\_C_s$ and $^{\#4348}C_{66}\_C_{2v}$ serve as the addition parents for the enlargement from C_{66} to C_{68}. Interestingly, by C_2 addition, the two C_{66} isomers can both grow to two distinct experimentally synthesized C_{68} structures. In the case of $^{\#4348}C_{66}\_C_{2v}$, the insertion product with the least fused pentagons is $^{\#6094}C_{68}\_C_s$, which behaves two as pentagon pairs (the lowest number of pentagon pairs among 6332 classical C_{68} isomers) and was observed in the formed $C_{68}Cl_8$ lately by in situ chlorination.[13] As shown in Scheme 6, the enlargement process occurs on a typical 5/6/5 segment in $^{\#4348}C_{66}\_C_{2v}$, and based on our calculations, the singlet−triplet splitting energy ΔE_{st} for $^{\#6094}C_{68}\_C_s$ is as large as −0.40 eV, suggesting that the ground spin state for the molecule is an open-shell triplet state rather than a singlet state. Our results indicate that the growth needs to overcome the energy barrier of 0.89 eV (reaction rate is 1.7

Scheme 6. C_2 Addition from $^{\#4348}C_{66}\_C_{2v}$ to $^{\#6094}C_{68}\_C_s$[a,b,c]

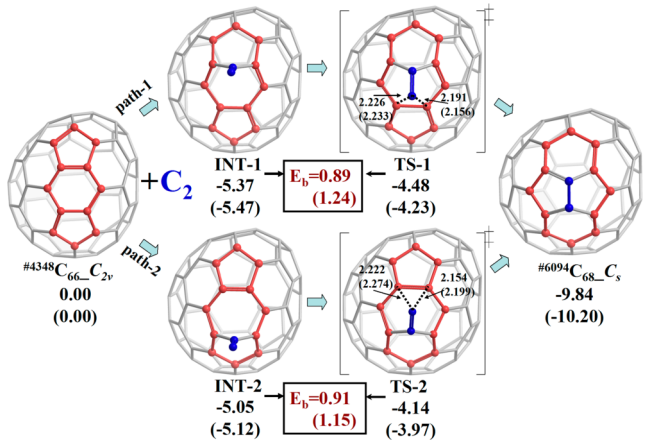

[a]E_b indicates the energy barrier. [b]Energies are given in eV, and C−C distances are in units of Å. [c]Energies and bond distances in brackets denote the triplet results.

× 10^{11} s^{-1} at 2500 K) in the singlet state or 1.24 eV (with the reaction rate of 3.8 × 10^{10} s^{-1}) in the triplet state. Moreover, as shown in Table 1, because the reactant, the stick-like intermediate, and the product are energetically favorable in the triplet state, the growth from $^{\#4348}C_{66}\_C_{2v}$ to $^{\#6094}C_{68}\_C_s$ is treated as a spin-unrestricted reaction in the triplet PES. Besides, similar with $^{\#3457}C_{64}\_C_2$, the two pentagon pairs in $^{\#6094}C_{68}\_C_s$ are also equivalent. Hence $^{\#4348}C_{66}\_C_{2v}$ is the only suitable addition parent for $^{\#6094}C_{68}\_C_s$, which indicates the importance of $^{\#4348}C_{66}\_C_{2v}$ in fullerene growth.

While acting as the parent molecule of growth, the C_2 addition on $^{\#4169}C_{66}\_C_s$ has already been uncovered. By one step of C_2 insertion on the fragment 5/6/6 (see Scheme 7), a

Scheme 7. C_2 Addition from $^{\#4169}C_{66}\_C_s$ to Hepta-C_{68}[a,b]

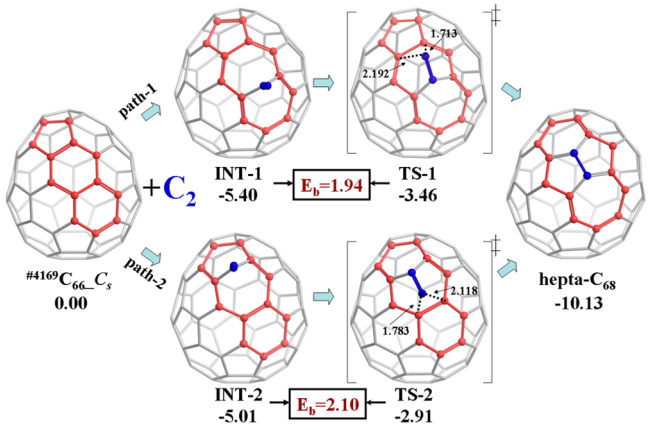

[a]E_b indicates the energy barrier. [b]Energies are given in eV, and C−C distances are in units of Å.

heptagon-containing nonclassical C_{68} fullerene (denotes as hepta-C_{68}) is yielded. Captured as chloride $C_{68}Cl_6$ by Tan and coworkers, the product has already been proved to be the most thermodynamically stable isomer above 2000 K.[16] However, although the structural connectivity of $^{\#4169}C_{66}\_C_s$ and hepta-C_{68} has already been revealed, detailed reaction mechanisms for the process from $^{\#4169}C_{66}\_C_s$ to hepta-C_{68} are still unknown. As those experimental scientists claimed, powerful evidence to

dx.doi.org/10.1021/jp3100766 | J. Phys. Chem. C 2013, 117, 2349−2357

elucidate the authentic heptagon road is needed.[16,50] Herein, for the first time, we studied the kinetic process of this heptagon road in the singlet spin state at the DFT level of theory because the ground states for the reactant and product are both singlet (ΔE_{st} for hepta-C_{68} is 0.72 eV). As shown in Scheme 7, the C_2 insertion is divided into two patterns according to the adsorption sites for the external C_2 dimer. In energy, the C_2 dimer is apt to adsorb on the [6,6] conjunction to form a more stable stick-like intermediate with the reaction energy of −5.40 eV. Moreover, the addition on the [6,6] bond (path-1) needs a lower reaction barrier of 1.94 eV, which is 0.16 eV lower than that on the [5,6] conjunction. Accordingly, path-1 in Scheme 7 is a preponderant reaction pathway in both kinetic and thermodynamic considerations, and the calculated reaction rate is 1.5×10^9 s^{-1} at 2500 K. Additionally, it is worthwhile to note that the activation barrier for this process is 1.01 eV lower than the other heptagon-involved fullerene, hepta-C_{62}, which causes a larger probability for hepta-C_{68} to be discovered experimentally.

C_{68}−C_{70}: SWT-Involved Growth. This is the last growth course we discussed in the report. However, different from the above-mentioned reaction pathways from C_{60} to C_{68}, structural analysis on $^{\#6094}C_{68}\_C_s$ and hepta-C_{68} suggests that neither of the two molecules can afford $^{\#8149}C_{70}\_D_{5h}$ by C_2 addition directly. Therefore, fullerene isomerization is unavoidable for the growth from C_{68} to C_{70}.

As shown in Scheme 8, by C_2 insertion on the 5/6/5 fragment of $^{\#6094}C_{68}\_C_s$, we found that the product is

Scheme 8. Growth from $^{\#6094}C_{68}\_C_s$ to $^{\#8149}C_{70}\_D_{5h}$ by C_2 Addition and Stone−Wales Transformation[a,b,c]

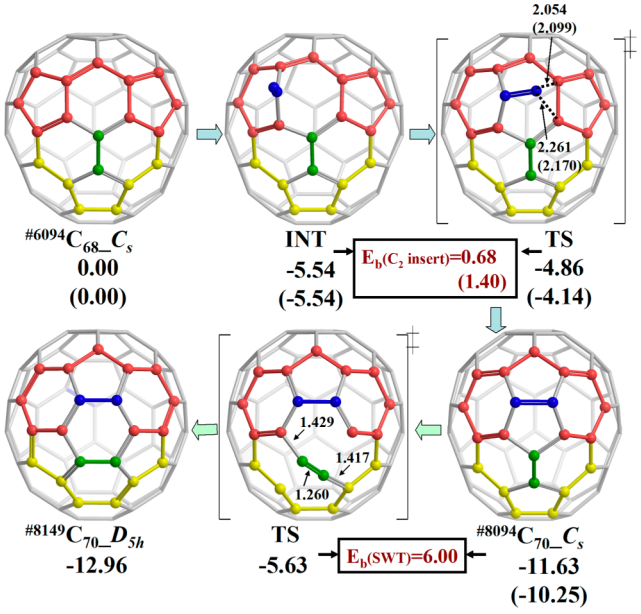

[a] E_b indicates the energy barrier. [b] Energies are given in eV, and C−C distances are in units of Å. [c] Energies and bond distances in brackets denote the triplet results.

$^{\#8094}C_{70}\_C_s$ (with the ΔE_{st} of 0.98 eV), which has a pentagon pair. Additionally, $^{\#8094}C_{70}\_C_s$ is also the most stable C_2 addition product from $^{\#6094}C_{68}\_C_s$. The energy barrier for the addition is 1.40 eV (0.68 eV) in the triplet (singlet) PES, revealing that the formation of $^{\#8094}C_{70}\_C_s$ is facilitated. However, to obtain the IPR-C_{70} ($^{\#8149}C_{70}\_D_{5h}$), one step of SWT (shown in Figure 1) is necessary. The activation barrier for the SWT is as high as 6.00 eV at the B3LYP/6-31G(d) level of theory, hence this step of SWT serves as the rate-determining step of C_{68}−C_{70} process. In the case of hepta-C_{68}, the enlargement to singlet $^{\#8149}C_{70}\_D_{5h}$ (ΔE_{st} is 1.62 eV) has already been studied systematically. Among all possible routes, the most favorable mechanism is proposed by Tan et al., involving one step of C_2 insertion from hepta-C_{68} to $^{\#8144}C_{70}\_C_s$ (ΔE_{st} is 0.93 eV) as well as two steps of SWT (from $^{\#8144}C_{70}\_C_s$ to $^{\#8094}C_{70}\_C_s$ to $^{\#8149}C_{70}\_D_{5h}$).[16,45] Herein we recalculated these processes at the B3LYP/6-31G(d) level. As shown in Scheme 9, the energy barriers of the three

Scheme 9. Growth from Hepta-C_{68} to $^{\#8149}C_{70}\_D_{5h}$ by C_2 Addition and Stone−Wales Transformation[a,b]

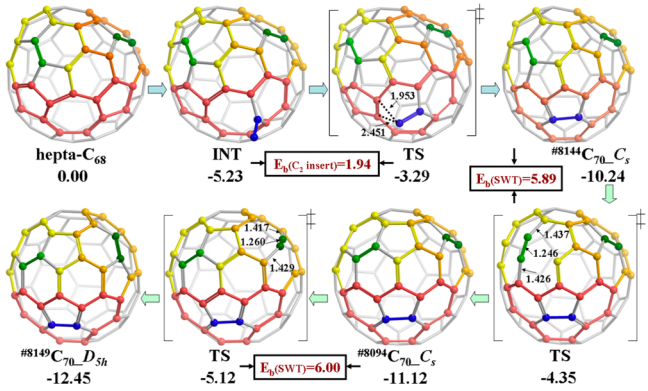

[a] E_b indicates the energy barrier. [b] Energies are given in eV, and C−C distances are in units of Å.

reactions are 1.94, 5.89, and 6.00 eV, respectively. Consequently, similar to the growth from $^{\#6094}C_{68}\_C_s$, the isomerization from $^{\#8094}C_{70}\_C_s$ to $^{\#8149}C_{70}\_D_{5h}$ determines the whole reaction rate. On the basis of the Arrhenius formula, the reaction rate of SWT is 2.6×10^1 at 2500 K, hence although the formation of IPR-C_{70} ($^{\#8149}C_{70}\_D_{5h}$) cannot be explained simply by C_2 additions, the targeted molecule can still be accomplished at high temperatures by SWT.

Overall, the complete growth channel from $^{\#1812}C_{60}\_I_h$ to $^{\#8149}C_{70}\_D_{5h}$ is represented in Scheme 10. Structurally, we found that various addition models are included in the growth, not only the traditional Endo−Kroto patch but also additions on the 5/6/6 fragment of IPR-C_{60} and heptagonal rings of nonclassical fullerenes. Energetically, as listed in Table 1, all addition reactions are highly exothermic with the activation barriers lower than 3 eV, and generally all C_2 insertions exhibit a relative consistency in both thermodynamic and kinetic controls. The C_2 insertion on $^{\#1812}C_{60}\_I_h$ possesses the highest energy barrier (2.95 eV) and the smallest exothermic reaction energy (−7.46 eV) among all discussed C_2 addition reactions. Accordingly, the formation of hepta-C_{62} is predicted to be the most difficult reaction. As illustrated in Scheme 10, the molecules labeled in red denote the synthesized pristine cages or chlorofullerenes in experiments, and the others have not hitherto been defined in laboratory. Our calculations supplied reasonable explanations on the discovery of those captured molecules and also theoretical supports on the unobserved structures of the growth channel. Without a doubt, we never exclude the possibility of other mechanisms and do believe that

dx.doi.org/10.1021/jp3100766 | J. Phys. Chem. C 2013, 117, 2349−2357

Scheme 10. Growth Pathway from $^{\#1812}C_{60}\_I_h$ to $^{\#8149}C_{70}\_D_{5h}$.[a]

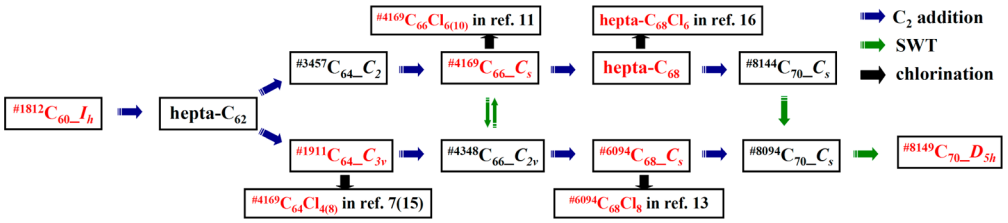

[a]Molecules labeled in red denote the synthesized pristine cages or chlorofullerenes.

different formation mechanisms (i.e., C_2 ejection and C_2 incorporation) can coexist under certain conditions.[25]

4. CONCLUSIONS

Fullerene growth from C_{60} to C_{70} was investigated by using DFT calculations. A thermodynamically and kinetically favorable pathway was proposed based on geometrical analysis and reaction PES survey. Our study demonstrates that the synthesized chlorofullerenes ($^{\#1812}C_{60}$, $^{\#1911}C_{64}$, $^{\#4169}C_{66}$, hepta-C_{68}, $^{\#6094}C_{68}$) are connected via successive C_2 addition reactions with negative formation energies as well as low barriers. Moreover, the existence of some undetected fullerene cages along the special growth route ($^{\#3457}C_{64}$, $^{\#4348}C_{66}$, $^{\#8094}C_{70}$, $^{\#8144}C_{70}$) is predicted for the first time. These theoretical results provide a reliable elucidation on the formation mechanism of pristine fullerenes and the exohedral derivatives, which are believed to be useful to find more new materials for promising applications.

■ ASSOCIATED CONTENT

Supporting Information

Full citations of refs 5−7, 11, 12, and 32. This material is available free of charge via the Internet at http://pubs.acs.org.

■ AUTHOR INFORMATION

Corresponding Author

*E-mail: xzhao@mail.xjtu.edu.cn.

Author Contributions

§These authors contributed equally.

Author Contributions

The manuscript was written through contributions of all authors. All authors have given the final approval to current version of the manuscript.

Notes

The authors declare no competing financial interest.

■ ACKNOWLEDGMENTS

This work has been financially supported by National Natural Science Foundation of China (21171138, 20673081) and partially by the National Key Basic Research Program of China (2012CB720904).

■ REFERENCES

(1) Kroto, H. W.; Heath, J. R.; O'Brien, S. C.; Curl, R. F.; Smalley, R. E. C_{60}: Buckminsterfullerene. *Nature* **1985**, *318*, 162−163.

(2) Krätschmer, W.; Lamb, L. D.; Fostiropoulos, K.; Huffman, D. R. Solid C_{60}: a New Form of Carbon. *Nature* **1990**, *347*, 354−358.

(3) Kroto, H. W. The Stability of the Fullerenes C_n, with n = 24, 28, 32, 36, 50, 60 and 70. *Nature* **1987**, *329*, 529−531.

(4) Xie, S. Y.; Gao, F.; Lu, X.; Huang, R. B.; Wang, C. R.; Zhang, X.; Liu, M. L.; Deng, S. L.; Zheng, L. S. Capturing the Labile Fullerene[50] as $C_{50}Cl_{10}$. *Science* **2004**, *304*, 699.

(5) Tan, Y. Z.; Han, X.; Wu, X.; Meng, Y. Y.; Zhu, F.; Qian, Z. Z.; Liao, Z. J.; Chen, M. H.; Lu, X.; Xie, S. Y.; et al. An Entrant of Smaller Fullerene: C_{56} Captured by Chlorines and Aligned in Linear Chains. *J. Am. Chem. Soc.* **2008**, *130*, 15240−15241.

(6) Tan, Y. Z.; Liao, Z. J.; Qian, Z. Z.; Chen, R. T.; Wu, X.; Liang, H.; Han, X.; Zhu, F.; Zhou, S. J.; Zheng, Z.; et al. Two I_h-symmetry-breaking C_{60} Isomers Stabilized by Chlorination. *Nat. Mater.* **2008**, *7*, 790−794.

(7) Han, X.; Zhou, S. J.; Tan, Y. Z.; Wu, X.; Gao, F.; Liao, Z. J.; Huang, R. B.; Feng, Y. Q.; Lu, X.; Xie, S. Y.; et al. Crystal Structures of Saturn-Like $C_{50}Cl_{10}$ and Pineapple-Shaped $C_{64}Cl_4$: Geometric Implications of Double- and Triple-Pentagon-Fused Chlorofullerenes. *Angew. Chem., Int. Ed.* **2008**, *47*, 5340−5343.

(8) Tan, Y. Z; Xie, S. Y.; Huang, R. B.; Zheng, L. S. The Stabilization of Fused-Pentagon Fullerene Molecules. *Nat. Chem.* **2009**, *1*, 450−460.

(9) Tan, Y. Z.; Li, J.; Zhou, T.; Feng, Y. Q.; Lin, S. C.; Lu, X.; Zhan, Z. P.; Xie, S. Y.; Huang, R. B.; Zheng, L. S. Pentagon-Fused Hollow Fullerene in C_{78} Family Retrieved by Chlorination. *J. Am. Chem. Soc.* **2010**, *132*, 12648−12652.

(10) Ioffe, I. N.; Chen, C.; Yang, S.; Sidorov, L. N.; Kemnitz, E.; Troyanov, S. I. Chlorination of C_{86} to $C_{84}Cl_{32}$ with Nonclassical Heptagon-Containing Fullerene Cage Formed by Cage Shrinkage. *Angew. Chem., Int. Ed.* **2010**, *49*, 4784−4787.

(11) Tan, Y. Z.; Li, J.; Zhu, F.; Han, X.; Jiang, W. S.; Huang, R. B.; Zheng, Z.; Qian, Z. Z.; Chen, R. T.; Liao, Z. J.; et al. Chlorofullerenes Featuring Triple Sequentially Fused Pentagons. *Nat. Chem.* **2010**, *2*, 269−273.

(12) Zhou, T.; Tan, Y. Z.; Shan, G. J.; Zou, X. M.; Gao, C. L.; Li, X.; Li, K.; Deng, L. L.; Huang, R. B.; Zheng, L. S.; et al. Retrieving the Most Prevalent Small Fullerene C_{56}. *Chem.—Eur. J.* **2011**, *17*, 8529−8532.

(13) Amsharov, K. Y.; Ziegler, K.; Mueller, A.; Jansen, M. Capturing the Antiaromatic $^{\#6094}C_{68}$ Carbon Cage in the Radio-Frequency Furnace. *Chem.—Eur. J.* **2012**, *18*, 9289−9293.

(14) Mueller, A.; Ziegler, K.; Amsharov, K. Y.; Jansen, M. In Situ Synthesis of Chlorinated Fullerenes by the High-Frequency Furnace Method. *Eur. J. Inorg. Chem.* **2011**, 268−272.

(15) Shan, G. J.; Tan, Y. Z.; Zhou, T.; Zou, X. M.; Li, B. W.; Xue, C.; Chu, C. X.; Xie, S. Y.; Huang, R. B.; Zhen, L. S. $C_{64}Cl_8$: A Strain-Relief Pattern to Stabilize Fullerenes Containing Triple Directly Fused Pentagons. *Chem. Asian J.* **2012**, *7*, 2036−2039.

(16) Tan, Y. Z.; Chen, R. T.; Liao, Z. J.; Li, J.; Zhu, F.; Lu, X.; Xie, S. Y.; Li, J.; Huang, R. B.; Zheng, L. S. Carbon Arc Production of Heptagon-Containing Fullerene. *Nature Comm.* **2011**, *2*, 420.

(17) Yang, S.; Wei, T.; Kemnitz, E.; Troyanov, S. I. Four Isomers of C_{96} Fullerene Structurally Proven as $C_{96}Cl_{22}$ and $C_{96}Cl_{24}$. *Angew. Chem., Int. Ed.* **2012**, *51*, 8239−8242.

(18) Heath, J. R. In Fullerenes-Synthesis, Properties, and Chemistry of Large Carbon Clusters. *ACS Symp. Ser.* **1992**, *481*, 1−22.

(19) Curl, R. F.; Smalley, R. E. Probing C-60. *Science* **1988**, *242*, 1017−1022.

(20) Smalley, R. E. Self-Assembly of the Fullerenes. *Acc. Chem. Res.* **1992**, *25*, 98−105.
(21) Wakabayashi, T.; Achiba, Y. A Model for the C_{60} and C_{70} Growth Mechanism. *Chem. Phys. Lett.* **1992**, *190*, 465−468.
(22) Von Helden, G.; Gotts, N. G.; Bowers, M. T. Experimental Evidence for the Formation of Fullerenes by Collisional Heating of Carbon Rings in the Gas Phase. *Nature* **1993**, *363*, 60−63.
(23) Irle, S.; Zheng, G.; Wang, Z.; Morokuma, K. The C_{60} Formation Puzzle "Solved": QM/MD Simulations Reveal the Shrinking Hot Giant Road of the Dynamic Fullerene Self-Assembly Mechanism. *J. Phys. Chem. B* **2006**, *110*, 14531−14545.
(24) Budyka, M. F.; Zyubina, T. S.; Ryabenko, A. G.; Muradyan, V. E.; Esipov, S. E.; Cherepanova, N. I. Is C_2 Cluster Ingested by Fullerene C_{60}? *Chem. Phys. Lett.* **2002**, *354*, 93−99.
(25) Saha, B.; Irle, S.; Morokuma, K. Hot Giant Fullerenes Eject and Capture C_2 Molecules: QM/MD Simulations with Constant Density. *J. Phys. Chem. C* **2011**, *115*, 22707−22716.
(26) Shvartsburg, A. A.; Hudgins, R. R.; Dugourd, P.; Gutierrez, R.; Frauenheim, T.; Jarrold, M. F. Observation of "Stick" and "Handle" Intermediates along the Fullerene Road. *Phys. Rev. Lett.* **2000**, *84*, 2421−2424.
(27) Endo, M.; Kroto, H. W. Formation of Carbon Nanofibers. *J. Phys. Chem.* **1992**, *96*, 6941−6944.
(28) Murry, R. L.; Strout, D. L.; Odom, G. K.; Scuseria, G. E. Role of sp^3 Carbon and 7-Membered Rings in Fullerene Annealing and Fragmentation. *Nature* **1993**, *366*, 665−667.
(29) Van Orden, A.; Saykally, R. J. Small Carbon Clusters: Spectroscopy, Structure, and Energetics. *Chem. Rev.* **1998**, *98*, 2313−2358.
(30) Dunk, P. W.; Kaiser, N. K.; Hendrickson, C. L.; Quinn, J. P.; Ewels, C. P.; Nakanishi, Y.; Sasaki, Y.; Shinohara, H.; Marshall, A. G.; Kroto, H. W. Closed Network Growth of Fullerenes. *Nat. Commun.* **2012**, *3*, 855.
(31) Dang, J. S.; Wang, W. W.; Zheng, J. J.; Zhao, X.; Ōsawa, E.; Nagase, S. Fullerene Genetic Code: Inheritable Stability and Regioselective C_2 Assembly. *J. Phys. Chem. C* **2012**, *116*, 16233−16239.
(32) Frisch, M. J.; Trucks, G. W.; Schlegel, H. B.; Scuseria, G. E.; Robb, M. A.; Cheeseman, J. R.; Scalmani, G.; Barone, V.; Mennucci, B.; Petersson, G. A. et al. *Gaussian 09*, Revision A.02; Gaussian, Inc.: Wallingford, CT, 2009.
(33) Becke, A. D. Density-Functional Thermochemistry. III. The Role of Exact Exchange. *J. Chem. Phys.* **1993**, *98*, 5648−5652.
(34) Lee, C.; Yang, W.; Parr, R. G. Development of the Colic-Salvetti Correlation-Energy Formula into a Functional of the Electron Density. *Phys. Rev. B* **1988**, *37*, 785−789.
(35) Hariharan, P. C.; Pople, J. A. Influence of Polarization Functions on MO Hydrogenation Energies. *Theor. Chim. Acta* **1973**, *28*, 213−222.
(36) Zhao, Y.; Truhlar, D. G. The M06 Suite of Density Functionals for Main Group Thermochemistry, Thermochemical Kinetics, Noncovalent Interactions, Excited States, and Transition Elements: Two New Functionals and Systematic Testing of Four M06-class Functionals and 12 Other Functionals. *Theor. Chem. Acc.* **2008**, *120*, 215−241.
(37) Fowler, P. W.; Manolopoulos, D. E. An Atlas of Fullerenes; Clarendon Press: Oxford, U.K., 1995.
(38) Stone, A. J.; Wales, D. J. Theoretical Studies of Icosahedral C_{60} and Some Related Species. *Chem. Phys. Lett.* **1986**, *128*, 501−503.
(39) Yoshida, M.; Osawa, E. Formalized Drawing of Fullerene Nets. 2. Applications to Mapping of Pyracylene Rearrangments, C_2-Insertion/Elimination Pathways, and Leapfrog/Carbon Cylinder Operations. *Bull. Chem. Soc. Jpn.* **1995**, *68*, 2083−2092.
(40) Ōsawa, E.; Ueno, H.; Yoshida, M.; Slanina, Z.; Zhao, X.; Nishiyama, M.; Saito, H. Combined Topological and Energy Analysis of the Annealing Process in Fullerene Formation. Stone−Wales Interconversion Pathways Among IPR Isomers of Higher Fullerenes. *J. Chem. Soc., Perkin Trans. 2* **1998**, 943−950.
(41) Wang, W.; Dang, J.; Zhao, X. Role of Four-Membered Rings in C_{32} Fullerene Stability and Mechanisms of Generalized Stone−Wales Transformation: a Density Functional Theory Investigation. *Phys. Chem. Chem. Phys.* **2011**, *13*, 14629−14635.
(42) Nardelli, M. B.; Yakobson, B. I.; Bernholc, J. Brittle and Ductile Behavior in Carbon Nanotubes. *Phys. Rev. Lett.* **1998**, *81*, 4656−4659.
(43) Ma, J.; Alfè, D.; Michaelides, A.; Wang, E. Stone−Wales Defects in Graphene and Other Planar sp^2-bonded Materials. *Phys. Rev. B* **2009**, *80*, 033407.
(44) Wang, W. W.; Dang, J. S.; Zheng, J. J.; Zhao, X.; Ōsawa, E.; Nagase, S. Metal-Promoted Restoration of Defective Graphene. *J. Mater. Chem.* **2012**, *22*, 16370−16375.
(45) Wang, W. W.; Dang, J. S.; Zheng, J. J.; Zhao, X. Heptagons in C_{68}: Impact on Stabilities, Growth, and Exohedral Derivatization of Fullerenes. *J. Phys. Chem. C* **2012**, *116*, 17288−17293.
(46) Qian, W.; Chuang, S. C.; Amador, R. B.; Jarrosson, T.; Sander, M.; Pieniazek, S.; Khan, S. I.; Rubin, Y. Synthesis of Stable Derivatives of C_{62}: The First Nonclassical Fullerene Incorporating a Four-Membered Ring. *J. Am. Chem. Soc.* **2003**, *125*, 2066−2067.
(47) Cui, Y. H.; Chen, D. L.; Tian, W. Q.; Feng, J. K. Structures, Stabilities, and Electronic and Optical Properties of C_{62} Fullerene Isomers. *J. Phys. Chem. A* **2007**, *111*, 7933−7939.
(48) Bettinger, H. F.; Yakobson, B. I.; Scuseria, G. E. Scratching the Surface of Buckminsterfullerene: the Barriers for Stone−Wales Transformation Through Symmetric and Asymmetric Transition States. *J. Am. Chem. Soc.* **2003**, *125*, 5572−5580.
(49) Wang, C. R.; Kai, T.; Tomiyama, T.; Yoshida, T.; Kobayashi, Y.; Nishibori, E.; Takata, M.; Sakata, M.; Shinohara, H. Materials Science: C_{66} Fullerene Encaging a Scandium Dimer. *Nature* **2000**, *408*, 426−427.
(50) Hernandez, E.; Ordejon, P.; Terrones, H. Fullerene Growth and the Role of Nonclassical Isomers. *Phys. Rev. B* **2001**, *63*, 193403.